Probe measurements of the space potential in a radio frequency discharge

V. A. Godyak and R. B. Piejak
GTE Laboratories Incorporated, 40 Sylvan Road, Waltham, Massachusetts 02254

(Received 2 April 1990; accepted for publication 6 June 1990)

The dc and radio frequency (rf) components (and harmonics) of the probe potential have been measured in the midplane of a 13.56-MHz parallel-plane rf discharge in argon over a wide range of discharge voltages and at gas pressures between 10 mTorr and 1.0 Torr. rf potential measurements were made with different input capacitances to determine the true magnitude of the rf plasma potential and the probe capacitance. For a symmetrically driven rf discharge, the rf plasma potential V_{rf} is mainly composed of the second harmonic of the driving voltage V_{dr} over a wide range of gas pressures. For high values of V_{dr}, $V_{rf} \approx 0.1\ V_{dr}$ while the dc probe potential V_{dc} is about $0.4\ V_{dr}$. These results are in good agreement with corresponding theoretical predictions found in the literature. For an asymmetrically driven rf discharge with equal electrode area, the rf plasma potential has an additional fundamental harmonic component equal to half the rf driving voltage. Values of rf plasma potential and probe capacitance given here allow us to specify the requirements on probe circuitry for different kinds of probe measurements in rf discharges.

I. INTRODUCTION

A general problem encountered with probe diagnostics in a radio frequency (rf) discharge plasma is the occurrence of a rf voltage component Φ across the probe sheath. This voltage is due to an oscillation in the plasma potential with respect ground, V_{rf}. The presence of Φ leads to distortion in the probe characteristic because of rectification in the nonlinear probe sheath, and this results in an incorrect determination of the plasma parameters. This has been widely discussed in the literature.[1–4]

To avoid probe-measurement distortion in a rf discharge plasma, Φ must be minimized through proper design of the probe and the probe circuitry. A general approach in making an undistorted probe measurement of the plasma potential (both dc and rf components) is to minimize the ratio of the probe-sheath impedance, Z_{sh}, to the total rf impedance of the external probe circuitry, Z_c. By following this approach the rf plasma potential is almost entirely across Z_c allowing the probe to track the rf plasma potential with virtually no rf voltage across the probe sheath.

The condition $|Z_c| \gg |Z_{sh}|$ has to be satisfied to directly measure the rf plasma potential V_{rf} with accuracy of $|Z_c/Z_{sh}|$. To obtain practically undistorted probe characteristics,[5,6] the following condition has to be fulfilled:

$$|Z_{sh}/Z_c| \leqslant (0.3\text{–}0.5)\, T_e/V_{rf}, \tag{1}$$

where T_e is the electron temperature in volts.

Thus, the plasma potential V_{rf} (for each frequency component) and the probe impedance Z_{sh} (at each frequency) must be known to determine an acceptable value of the probe circuit impedance for accurate probe measurements in a rf discharge plasma.

To minimize the ratio Z_{sh}/Z_c, it is obvious that Z_{sh} should be minimized and Z_c should be maximized. Z_{sh} may be minimized by enlarging the probe surface,[7] shunting the probe sheath with an auxiliary (large) electrode[8,9] or by using an emissive probe[6,10,11] that is closely coupled with the rf plasma. However, these techniques are limited by the introduction of a significant plasma density distortion in the vicinity of a large probe when its size is comparable to, or larger than, the electron mean free path λ_e.[12] To maximize Z_c, the rf impedance of the external circuitry should be made as large as possible.[7,13,14] Attempts to maximize the rf circuit impedance are limited by the input capacitance in the tip of the rf voltage probe, which is difficult to make less than 1 pF. In practice, these two limitations make it difficult to attain a ratio of Z_{sh}/Z_c that is less than 10% and 20% which is, indeed, the accuracy of the aforementioned measurements[7,13,14] of V_{rf}. It should also be noted that in some works[7,14,15] only the plasma potential oscillation at the fundamental frequency was considered, although there are significant higher-order harmonics in the rf plasma potential that have been demonstrated in experiments[8,16] and in rf discharge modeling.[17–19]

The main motivation of the present work is to specify values of the probe circuit impedance Z_c and sheath impedance Z_{sh} that satisfy the inequality (1), thereby making it possible to make accurate measurements of the probe characteristics in capacitive rf discharges. For this purpose the plasma potential (dc and rf components) along with the probe impedance are measured at the midplane of a symmetrically driven rf discharge over a wide range of gas pressures and rf discharge voltages.

The measurements show that in a symmetrically driven rf discharge, the rf component of the plasma potential consists mainly of the second harmonic of the driving frequency. Measured values of V_{rf} and V_0 (the dc component of the plasma potential) are compared with corresponding results found from rf discharge modeling and are demonstrated to be in good agreement. Data from the measurement of the magnitude of the spectral components of V_{rf} have been obtained for symmetric and asymmetric discharge excitation and, along with measurements of Z_c, they can be used in a

 0021-8979/90/193157-06$03.00

probe circuit design to assure the measurement of undistorted probe characteristics.

II. SYSTEM DESCRIPTION

This discharge system has been described in detail elsewhere,[20] so only a brief description will be given here. Measurements were made in a capacitively coupled, parallel-plate, symmetric, rf discharge enclosing the ends of a pyrex glass cylinder with a 14.2 cm i.d. The electrodes were aluminum with an electrode spacing of 6.7 cm. A balanced matcher was used to drive the discharge symmetrically such that the electrodes were 180° out of phase with each other when measured with respect to ground. The electrode voltages were samples directly on the rf electrodes by two voltage dividers fed into a waveform analyzer. The advantage of such a driving scheme is a reduction in the amplitude of the rf space potential of the plasma relative to an identical discharge driven single ended with the other electrode grounded. When driven symmetrically each rf electrode was tied to ground through a rf choke, as shown in Fig. 1.

The dc and rf components of the plasma potential were measured with a floating wire loop probe axially centered in the midplane of the discharge. The wire has a 0.125 mm radius and has a circular shape with a 6.0 cm diameter. Having a long wire with its radius smaller than an electron mean free path, a large probe surface area is attained without plasma density distortion about the wire. A wire extending normally to the loop and in the same plane is fed through a glass to metal feedthrough which is held vacuum tight by an o-ring fitting as shown in Fig. 2. The overall length of the wire in contact with the plasma is about 22 cm with an overall surface area of about 1.8 cm^2. Upon exiting the discharge chamber the probe is immediately terminated in the tip of a 100:1 capacitive voltage divider with an input capacitance $C_1 = 1.5$ pF and is fed to a 16-bit accuracy, 1-GHz bandwidth, waveform analyzer. The dc plasma potential (actually the dc floating potential, V_{dc}) was measured through a low capacitance ($\approx$0.04 pF) miniature resistor (1 MΩ) connected in series with the probe. This resistor is located where the probe exits the discharge chamber and isolates the probe from the capacitance of the dc voltmeter. Note that under conditions of the experiment, with the driving frequency $f = 13.56$ MHz being much higher than the ion plasma frequency, the impedance of the floating probe actually is determined by the probe sheath capacitance C_{sh}, i.e., $|Z_{sh}| = (\omega C_{sh})^{-1}$, and thus

$$Z_{sh}/Z_c = C_1/C_{sh}. \tag{2}$$

To measure the rf plasma potential along with the probe sheath capacitance, two successive voltage measurements are made, with two different input capacitances in the voltage divider, $C_{in} = C_1 = 1.5$ pF and $C_{in} = C_2 = 6.5$ pF $= C_1 + 5$ pF as shown in Fig. 3. Having readings of voltage V_1 and V_2 corresponding to input capacitances, C_1 and C_2, the following expressions can be evaluated for the true rf plasma potential V_{rf} and the probe sheath capacitance C_{sh} from Fig. 3:

$$V_{rf} = V_1 V_2 (C_2 - C_1)/(C_2 V_2 - C_1 V_1), \tag{3}$$

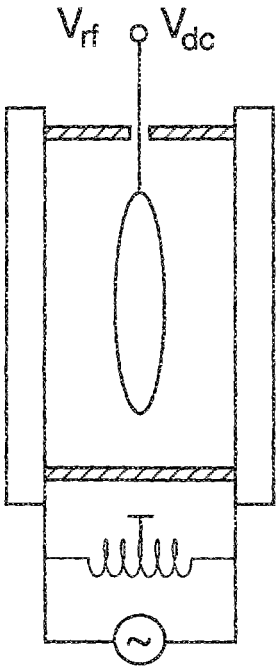

FIG. 1. Simplified diagram of a symmetric discharge system and probe potential measurement configuration.

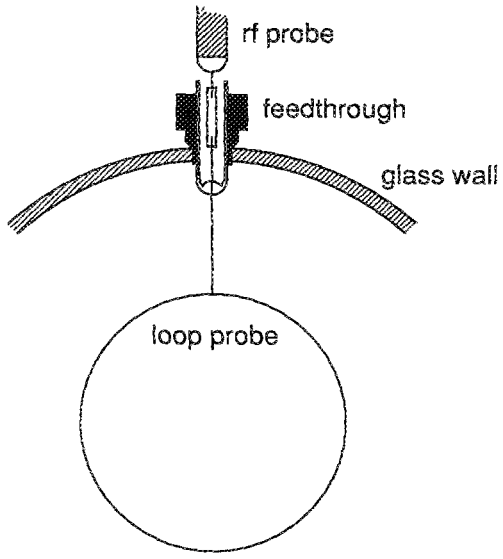

FIG. 2. Diagram of probe feedthrough into discharge chamber.

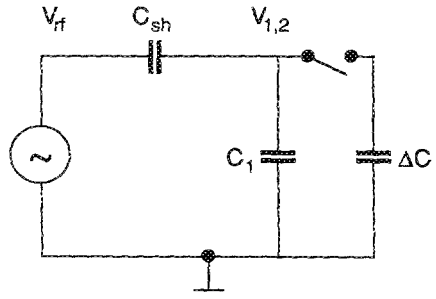

FIG. 3. Circuit diagram for rf potential measurement in rf discharge.

$$C_{sh} = (C_2 V_2 - C_1 V_1)/(V_1 - V_2). \quad (4)$$

From these equations it appears that this method of measuring V_{rf} does not require an extremely large ratio of $C_{1,2}/C_{sh}$ to achieve accurate measurements, however, the input capacitance of the voltage divider has to be small enough to prevent a significant rf current flow to the divider. This current may change the sheath capacitance due to the rf voltage drop across the probe sheath and rectification of this voltage by the probe sheath or it may change the rf plasma potential V_{rf} if it is comparable to the discharge rf current. Note that for the worst case of $C_{in} = C_2 = 6.5$ pF and at the lowest gas pressure, the rf probe current was between a fractional percentage and 5% of the discharge current. The influence of rf probe current on the probe capacitance the dc potential measurements will be discussed later after presenting the obtained results.

III. RESULTS AND DISCUSSION

All measurements were made in argon discharge at 13.56 MHz with a gas pressure between 10 mTorr and 1.0 Torr. Typical traces of the rf voltage measured with the input divider capacitance $C_1 = 1.5$ pF in the midplane for a symmetric and an asymmetric rf discharge are shown in Fig. 4, along with the driving voltage. An asymmetric discharge was made by allowing the driven electrode to float and grounding the opposite electrode. In both cases the total voltage across the electrode was 105 V (amplitude). In the case of the symmetric discharge, only the second harmonic component is apparent and its magnitude is about an order of magnitude less than the driving voltage. For the asymmetric discharge, the measured rf voltage is about one-half the driving voltage and is composed mainly of the driving frequency as would be expected for a discharge with equal area electrodes. Figure 5 shows the log of the magnitude of the measured plasma potential in the frequency domain for symmetric and asymmetric discharges. This figure gives more detail about the harmonic content found in the plasma for signal

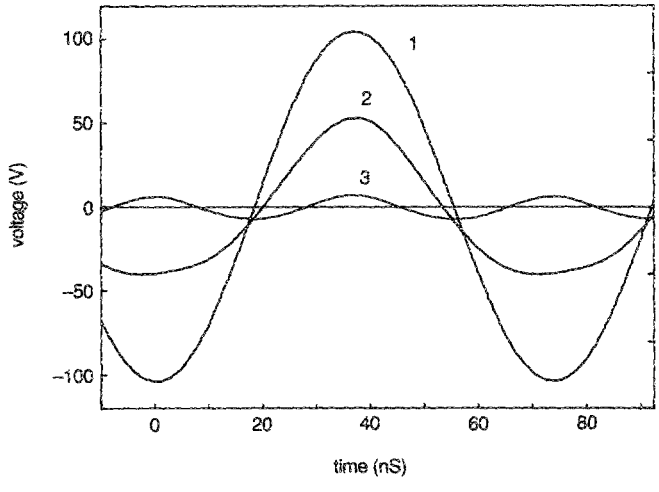

FIG. 4. A typical waveform of the rf driving voltage V_{dr} (denoted by 1) and the rf potential measured with a loop probe in an asymmetric rf discharge (2) and in a symmetric rf discharge (3).

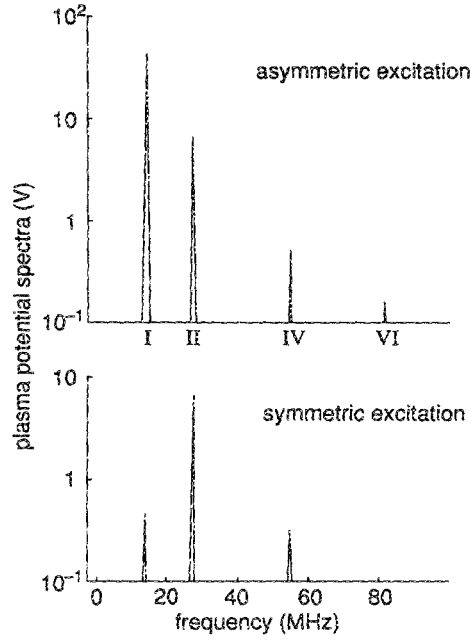

FIG. 5. The plasma potential spectra in a symmetric and an asymmetric rf discharge.

levels as low as -60 db with respect to the driving voltage. Note that the plasma potentials given in Figs. 4 and 5 are about 20% lower than their true values because of the finite ratio of C_{sh}/C_1 in these measurements. As shown in Fig. 5, the symmetric discharge appears to have a second and a fourth harmonic and a small fundamental component while the asymmetric discharge has a large fundamental component, a second harmonic equal to that seen in the symmetric discharge and small components in the fourth and the sixth harmonic. The appearance of the second harmonic in the symmetric discharge is due to electrode sheath modulation under the action of the rf discharge driving voltage while the fundamental harmonic is a consequence of either a small (about 1%) imbalance in the matcher or a slight misalignment of the loop probe from the midplane of the discharge. Ideally, for a balanced discharge an absence of odd harmonics is expected. For the widely used asymmetrically driven rf discharge configuration, and especially for discharges with different rf electrode areas, the plasma potential is normally enriched with higher-order harmonics. Although the nonlinearity in the rf discharge behavior generally grows with increasing electrode area ratio, the absolute value of the rf plasma potential (and thus the rf voltage across the rf sheath) generally decreases as the grounded electrode is enlarged with respect to the driven one.

The probe-sheath capacitance and the rf plasma potential (actually composed of mainly second harmonic) are shown in Figs. 6 and 7 for a symmetrically driven discharge at different gas pressures. The results are based on the probe potential measurements using formulas (2) and (3). As shown in Fig. 6, the probe sheath capacitance changes only slightly while the rf driving voltage and gas pressure vary by two orders of magnitude. The small change in the probe sheath capacitance is due to its logarithmic dependence on

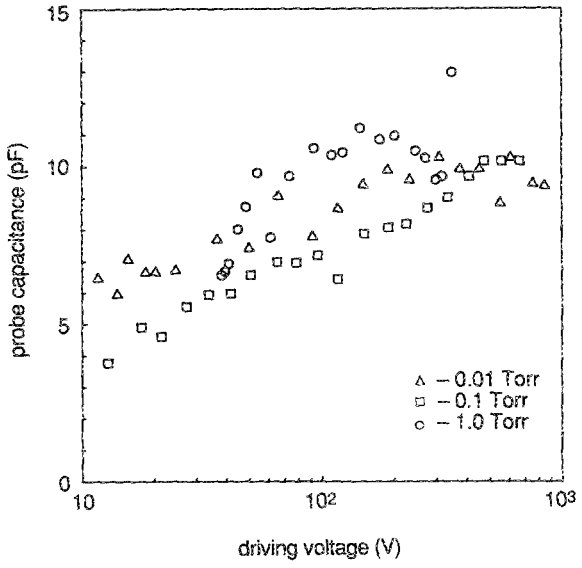

FIG. 6. Probe-sheath capacitance vs rf driving voltage.

the sheath width surrounding the probe. The capacitance of the wire loop can be evaluated using a formula for a cylindrical capacitor with length $L = \pi d$, where d is the diameter of the wire loop. The appropriate formula is $C_{sh} = 2\pi^2 d\epsilon_0 [\ln(1 + s/a)]^{-1}$, where a is the probe radius and s is the sheath width which for a floating probe is on the order of a few Debye lengths, $s = (2\text{–}3)\lambda_D$. Estimations of s based on electrical characteristic measurements[21] showed $s > a$ even for the highest plasma density. Therefore, an order-of-magnitude change is s (corresponding to a change of plasma density of two orders of magnitude) affects the probe sheath capacitance by a significantly smaller amount. The considerable scatter ($\pm 15\%$) in the observed values of C_{sh} given in Fig. 6 is a consequence of the rather large C_{sh}/C_{in} ratio at which the scatter in the capacitance is about C_{sh}/C_{in} times the measured scatter in the probe potential. For example, with $C_{sh} = 11$ pF and $C_{in} = C_i = 1.5$ pF, just a 2% dispersion in probe potential measurements corresponds to a 15% dispersion in the calculation of C_{sh}. Inaccuracy in determining C_{sh} actually affects the calculated values of the rf plasma potential very little as shown in Fig. 7. Here the amplitude of the second harmonic of the plasma rf potential V_{rf} is presented as a function of the driving voltage amplitude V_{dr} across the rf electrodes for different gas pressures. For large driving voltages, where the rf voltage drop across the plasma V_p can be neglected, the rf plasma potential in the plasma midplane is proportional to the driving voltage and has been measured to be about 8%–12% of V_{dr}. These values are close to those predicted theoretically for an ion-matrix model[17] and for a highly collisional[19] rf capacitive sheath model with large driving voltages and driving frequencies far greater than the ion plasma frequency. The corresponding values for the V_{rf}/V_{dr} ratio determined by these models are 9.8% and 9.7%, while a collisionless rf sheath model[18] yields 6.1% which is about twice less than observed here. It seems reasonable to consider the rf sheath in the present experiment as being collisional rather than collisionless because, even for the minimum gas pressure of 10 mTorr, the rf sheath width is still two to three times larger than the ion mean free path.

The dc potential of the floating loop probe was also measured for different gas pressures over a wide range of driving voltage as shown in Fig. 8. A qualitative diagram of the axial dc potential distribution is shown in Fig. 9 to facilitate the following discussion. The measured dc voltage V_{dc} consists of several terms (see Fig. 9):

$$V_{dc} = V_0 + V_{p0} - V_{f0} - \Delta V, \tag{5}$$

where V_0 is the dc voltage across the rf electrode sheath mainly due to rectification of the driving rf voltage; V_{p0} is the dc voltage drop between the midplane and the axial plasma boundary, $V_{p0} = T_e \ln(n_0/n_1) \approx (1\text{–}2)T_e$, and n_0 and n_1 are the plasma densities at the midplane and the plasma

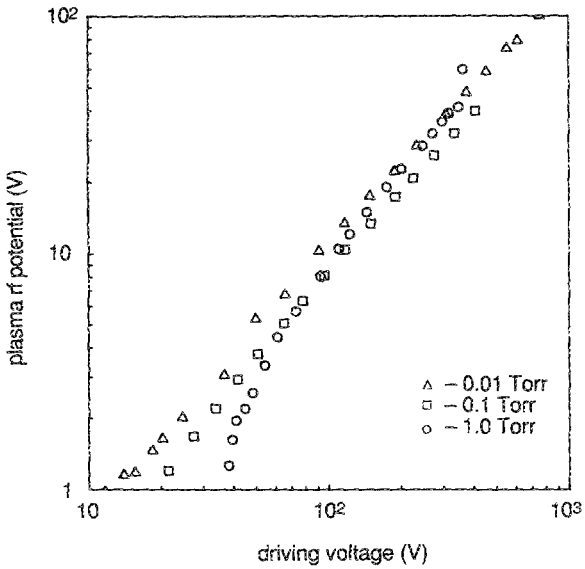

FIG. 7. rf potential vs driving voltage in a 13.56-MHz argon discharge at three gas pressures.

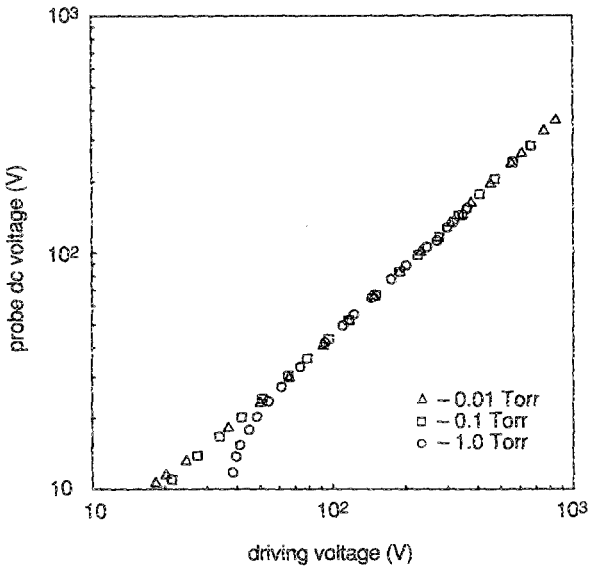

FIG. 8. dc probe potential vs rf driving voltage in a 13.56-MHz rf discharge at three gas pressures.

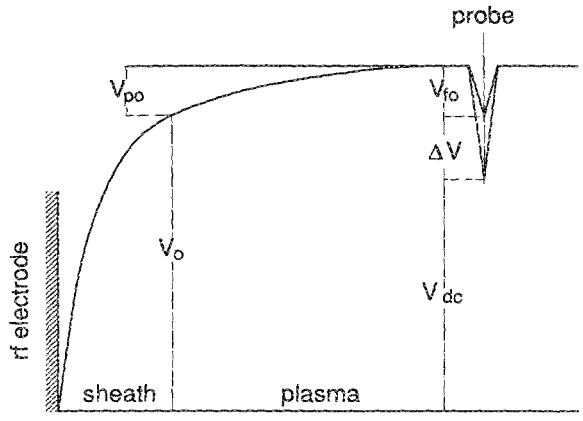

FIG. 9. Qualitative diagram of the dc potential distribution in a rf discharge.

boundary, respectively; V_{f0} is the undistorted floating probe voltage,

$$V_{f0} \approx \tfrac{1}{2} T_e \ln (M/2\pi m) - T_e \ln(a_1/a) \approx (3\text{–}4)\, T_e,$$

where M and m are the ion and the electron masses and a_1 is the effective ion collection radius, $a_1 \approx a + s$; and ΔV is the change in the floating probe voltage due to rectification of the rf probe voltage Φ, where $\Delta V \approx T_e \ln I_0 (\Phi/T_e)$ and I_0 is a modified Bessel function.

The true dc plasma potential $V_s = V_0 + V_{p0}$ is always somewhat higher than the measured voltage. For high rf driving voltages such that $V_{dr} \gg V_{f0} > T_e$, $V_s \approx V_0 \approx V_{dc} + \Delta V$. The floating voltage shift is governed by the rf component of the voltage across the probe sheath Φ which depends on the ratio of C_{sh}/C_{in} such that

$$\Phi = V_{rf} (1 + C_{sh}/C_{in})^{-1}. \tag{6}$$

The value of ΔV can be evaluated using (5) and (6). For (a typical case) $p = 0.1$ Torr and $V_{dr} = 500$ V from Figs. 6 and 7 we get $V_{rf} = 50$ V and $C_{sh} = 10$ pF. Assuming the electron temperature to be $T_e = 3$ V and taking the input capacitance to be $C_{in} = C_1 = 1.5$ pF, we obtain $\Phi_1 = 6.5$ V and $\Delta V_1 = 3$ V. For input capacitance $C_2 = 6.5$ pF we obtain $\Phi_2 = 20$ V and $\Delta V_2 = 14$ V. Thus, for this case with $V_{dr} = 500$ V and $V_{dc} = 200$ V the values of ΔV account for 1.5% and 7% of V_{dc} corresponding to an input capacitance of $C_1 = 1.5$ pF and $C_2 = 6.5$ pF.

The dc probe voltage measurements shown in Fig. 8 were performed through a resistor with low parasitic capacitance (a few hundredths of a pF) which corresponds to $C_{sh}/C_{in} > 100$ and $\Delta V < 0.02$ V. As shown in Fig. 8, the dc probe potential measurements for all three gas pressures fall on the same line which corresponds to a linear dependency where $V_{dc} = 0.4\, V_{dr}$. This is very close to the theoretical results found in the collisionless rf sheath model,[18] $V_{dc} = 0.414\, V_{dr}$, and in the highly collisional rf sheath model,[19] where $V_{dc} = 0.392\, V_{dr}$. Somewhat worse agreement is found with an ion matrix model rf sheath model[17] where $V_{dc} = 0.375\, V_{dr}$ and with a resistive sheath model[22,23] where $V_{dc} = V_{dr}/\pi = 0.318 V_{dr}$, although the last model is applicable to low-frequency discharges where the driving frequency is much lower than the ion plasma frequency.

At low driving voltages and high gas pressure (in Fig. 8 at $p = 1.0$ Torr) V_{dc} is smaller than $0.4 V_{dr}$. That is a result of the considerable rf voltage drop V_p across the plasma body with a corresponding reduction in the rf electrode sheath voltage V_e which actually determines the quantities V_{dc} and V_{rf}. The value of V_e is related to driving voltage V_{dr} by the equation[17]

$$V_e = V_p \omega/\nu_{eff} \pm (V_{dr}^2 - V_p^2)^{1/2}, \tag{7}$$

where ν_{eff} is the effective electron-neutral collision frequency.[17]

From (7) it can be seen that V_e drops sharply when V_{dr} approaches V_p while for the high voltages implicit in the above-mentioned models $V_e = V_{dr}$. Although the rectification effect on the loop probe only slightly affects the dc probe potential measurements in our experiment, it can significantly change the dc voltage across the probe sheath and thereby change its capacitance. Indeed, in the example above, with $V_{dr} = 500$ V and $C_{in} = C_2 = 6.5$ pF, the shift in the dc probe voltage $\Delta V = 14$ V is close or even larger than the undistorted probe floating voltage $V_{f0} \approx 4 T_e = 12$ V. This should not significantly change the probe sheath capacitance due to its logarithmic dependency on the probe sheath thickness (as discussed earlier), but even if C_{sh} should change considerably this would hardly affect the calculated rf plasma potential V_{rf}, providing that C_{in} remains small compared to C_{sh}.

IV. CONCLUSION

Having measured the magnitude of the rf plasma potential and the value of the probe capacitance, the minimum input impedance of the external probe circuitry Z_e needed for probe measurements with reasonable accuracy can be evaluated. The requirements on Z_e depend upon the objectives of the probe measurement. Typically, these are measurement of the rf and dc plasma potentials, measurements of the electron energy distribution function (EEDF), or measurement of the integral of the EEDF, i.e., a conventional Langmuir probe measurement.

Thus to make direct measurements of the plasma potential in high-voltage rf discharges with a relative error of $\epsilon \ll 1$, the input capacitance of the measuring device has to be smaller than ϵC_{sh} for the V_{rf} measurements and smaller than $4\epsilon C_{sh}$ for V_{dc} measurements. In a practical probe with a small probe holder to minimize plasma disturbance, the total probe capacitance is on the order of 1 pF and the tolerated input capacitance of the measurements circuit must be on the order of 0.01 pF. This can be achieved in the dc potential measurements using a low-capacitance miniature resistor as an rf filter. The practical approach to measure V_{rf} may be a combination of an enhanced probe coupling to the rf plasma along with V_{rf} measurements with different input capacitances as has been done here.

It is much more difficult to make undistorted EEDF or probe characteristic measurements. According to formula (1) and the values for the fundamental and second harmonic of the rf plasma potential (obtained in this work), V'_{rf} and V''_{rf}, an extremely large impedance in the probe circuitry (actually the impedance of a rf filter between the probe and

the probe circuitry) is needed for reliable plasma parameter measurements. To prevent probe characteristic distortion in an asymmetrical high-voltage rf discharge with equal electrode areas ($V'_{rf} \simeq 0.5 V_{dr}$ and $V''_{rf} \simeq 0.1 V_{dr}$) the appropriate filter must have the impedance Z'_c for the fundamental frequency ω, such that

$$Z'_c \geqslant 2Z'_{sh} V'_{rf}/T_e = V_{dr}/(T_e \omega C_{sh}), \tag{8}$$

and the impedance Z''_c for the second harmonic must be

$$Z''_c \geqslant 2Z''_{sh} V''_{rf}/T_e = 0.1 V_{dr}/(T_e \omega C_{sh}), \tag{9}$$

For a balanced symmetrically driven discharge, only the condition on the second harmonic is considered. This makes probe diagnostics in these discharge significantly easier since there is no component of the fundamental frequency and the input impedance restrictions are not as stringent ($Z''_c = 0.1 Z'_c$). To our knowledge the conditions (8) and (9), or the more general condition (1), have not been shown to be satisfied in any probe diagnostic experiments at 13.56 MHz that have been published in the last decade. This we believe is one of the reasons for so much controversy regarding basic plasma parameters obtained from these measurements.

ACKNOWLEDGMENT

The authors thank B. M. Alexandrovich for his help in this experiment.

[1]F. F. Chen, Modern Use of Langmuir Probe, Institute of Plasma Physics, Report No. 1PPY-750, Nagoya University, Nagoya, Japan, 1986.
[2]V. A. Godyak, *Soviet Radio Frequency Discharge Research* (Delphic Associates, Falls Church, VA 1986), Chap. 7, pp. 118–138.
[3]N. Hershkowitz, in *Plasma Diagnostics* (Academic–Harcourt, Brace & Javonovich, New York, 1989), Vol. 1, pp. 113–183.
[4]V. A. Godyak, *Measuring EEDF in Gas Discharge Plasmas*, in *NATO ASI Series E, Applied Science* (Kluwer, Dordrecht, 1990), Vol. 176, pp. 95–134.
[5]V. A. Godyak and O. A. Popov. Sov. Phys.—Tech. Phys. **22**, 461 (1977).
[6]V. A. Godyak and S. N. Oks, Sov. Phys.—Tech. Phys. **24**, 784 (1979).
[7]S. E. Savas and K. G. Donohoe, Rev. Sci. Instrum. **60**, 3391 (1989).
[8]R. R. J. Gagne and A. Cantin, J. Appl. Phys. **43**, 2639 (1972).
[9]A. Cantin and R. R. J. Gagne, Appl. Phys. Lett. **30**, 318 (1977).
[10]E. Y. Wang, N. Hershkowitz, T. Intrator, and C. Forest, Rev. Sci. Instrum. **57**, 2425 (1986).
[11]N. Hershkowitz and M. H. Cho, J. Vac. Sci. Technol. A **6**, 2054 (1988).
[12]J. F. Waymouth, J. Appl. Phys. **37**, 4493 (1966).
[13]J. B. O. Caughman, II, D. N. Ruzic, and D. J. Hoffman, J. Vac. Sci. Technol. A **7**, 1092 (1989).
[14]N. Benjamin, Rev. Sci. Instrum. **53**, 1541 (1982).
[15]J. L. Wilson, J. B. O. Caughman, II, P. L. Nguyen, and D. N. Ruzic, J. Vac. Sci. Technol. A **7**, 972 (1989).
[16]A. J. Hatch, in *Proceedings of the 5th International Conference on Phenomena in Ionized, Gases* (North-Holland, Amsterdam, 1962), Vol. 1, p. 747.
[17]V. A. Godyak, Sov. J. Plasma Phys. **2**, 78 (1976).
[18]M. Lieberman, Trans. IEEE Plasma Sci. **16**, 638 (1988).
[19]M. Lieberman, Trans. IEEE Plasma Sci. **17**, 65 (1989).
[20]V. A. Godyak, R. B. Piejak, and B. M. Alexandrovich, Rev. Sci. Instrum. (to be published).
[21]V. A. Godyak and R. B. Piejak, 42nd Annual Gaseous Electronics Conference, Palo Alto, CA paper J-1, 1989.
[22]V. A. Godyak, A. A. Kuzovnikov, V. P. Savinov, and A. Y. Sammani, J. Moscow Univ. Ser. 3, Phys. Astron. **2**, 126 (1968).
[23]V. A. Godyak and A. A. Kuzovnikov, Sov. J. Plasma Phys. **1**, 276 (1975).